RANDOM NOISE MONOPULSE RADAR SYSTEM FOR COVERT TRACKING OF TARGETS

Ram M. Narayanan
Department of Electrical Engineering
University of Nebraska
Lincoln, NE 68588-0511
Tel: (402) 472-5141; Fax: (402) 472-4732; email: ram@doppler.unl.edu

ABSTRACT

The University of Nebraska is currently developing a unique monopulse radar concept based on the use of random noise signal for covert tracking applications. This project is funded by the Missile Defense Agency (MDA). The advantage of this system over conventional frequency-modulated continuous wave (FMCW) or short pulse systems is its covertness resulting from the random waveform's immunity from interception and jamming. The system integrates a novel heterodyne correlation receiver with conventional monopulse architecture. Based on the previous work such as random noise interferometry, a series of theoretical analysis and simulations were conducted to examine the potential performance of this monopulse system. Furthermore, a prototype system is under development to exploit practical design aspects of phase comparison angle measurement. It is revealed that random noise monopulse radar can provide the same function as traditional monopulse radar, *i.e.*, implement range and angular estimation and tracking in real time. The bandwidth of random noise signal can be optimized to achieve the best range resolution as well as the angular accuracy.

INTRODUCTION

Phase comparison monopulse uses two apertures with displaced phase centers to locate the angle of arrival from scatters. The characteristic of this technique is its dependence on the phase information of received signals. When a random noise transmit waveform is employed, there will be much higher phase uncertainties compared to traditional waveforms due to its random nature. A phase coherent processing technique using the heterodyne correlation architecture has been developed and applied towards polarimetry[1], Doppler estimation[2], synthetic aperture (SAR) radar[3], and inverse SAR (ISAR)[4] with good success. The results obtained compare well with those obtained using conventional waveforms with the added advantage of covertness, *i.e.*, immunity from detection and jamming.

One application we have demonstrated that clearly suggests the use of this technique for angular tracking of targets is ultra-wideband (UWB) random noise interferometry. In our experiments, we showed that it was indeed possible to use the phase difference between spaced receiver antennas to locate a target in azimuth, while precise range information was obtained from the target delay. We have also developed the necessary analytical formulation for a clearer understanding of this technique together with its advantages and limitations[5].

Our recent results analyze the applicability of conventional phase-comparison monopulse techniques to the random noise radar system. A monopulse architecture based on sum-and-difference network was used to perform simulation studies. The transmit waveform was assumed to be bandlimited white noise, which was approximated as the summation of a large number of frequency components over the bandwidth, each component having a random amplitude. Received signals are passed through the sum-and-difference hybrid and mixed with a delayed replica of the transmit signal. The intermediate frequency (IF) outputs are routed through band pass filters following which a complex correlation operation is performed. This output provides information on the target direction dynamically. A detailed analysis shows that under ideal conditions, *i.e.,* flat frequency characteristics for the atmospheric propagation as well as for the target reflectance over the operating bandwidth, the output of the monopulse system is identical to that of the single frequency monopulse in the average sense.

ANTENNA SYSTEM

The antenna is the first component to process the received random noise signal plus uncorrelated system noise. Two special factors influence the performance of random noise monopulse antenna system. The first is signal bandwidth, and the second is the random fluctuations in signal phase and amplitude.

For narrowband systems, the antenna pattern is generally well characterized, and is considered invariant over the operating frequency range. However, a UWB waveform operates over a much wider fractional bandwidth, typically greater than 25%. The

Report Documentation Page

Report Date 29JUL2002	Report Type N/A	Dates Covered (from... to) -

Title and Subtitle Random Noise Monopulse Radar System for Covert Tracking of Targets	**Contract Number**
	Grant Number
	Program Element Number
Author(s)	**Project Number**
	Task Number
	Work Unit Number
Performing Organization Name(s) and Address(es) Department of Electrical Engineering University of Nebraska Lincoln, NE 68588-0511	**Performing Organization Report Number**
Sponsoring/Monitoring Agency Name(s) and Address(es)	**Sponsor/Monitor’s Acronym(s)**
	Sponsor/Monitor’s Report Number(s)
Distribution/Availability Statement Approved for public release, distribution unlimited	
Supplementary Notes See Also ADM201460. Papers from Unclassified Proceedings from the 11th Annual AAIA/MDA Technology Conference held in Monterey, CA from 29 Jul - 2 Aug 2002., The original document contains color images.	
Abstract	
Subject Terms	
Report Classification unclassified	**Classification of this page** unclassified
Classification of Abstract unclassified	**Limitation of Abstract** SAR
Number of Pages 9	

differences in the antenna patterns at different frequencies may introduce measurement errors. As an example, Figure 1 shows the amplitude pattern of a typical X-band horn antenna at 9 GHz, 10 GHz and 11 GHz. This simulation suggests that over a narrow angular region (±10°), the antenna patterns over the frequency range are essentially identical. However, the patterns are different beyond this region.

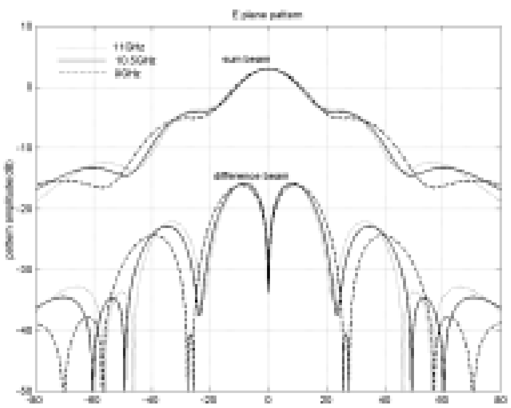

(a) E-plane pattern

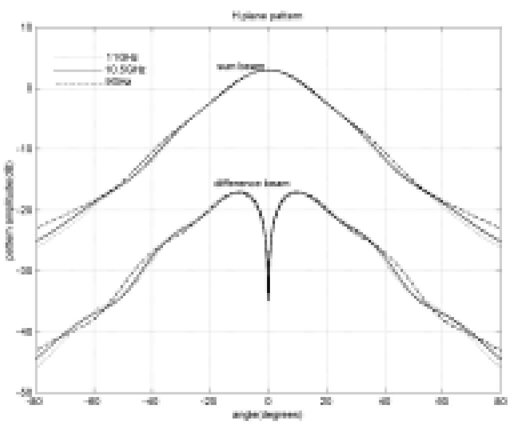

(b) H-plane pattern

Figure 1: Magnitude of pattern of an X-band horn antenna at different frequencies (9, 10, and 11 GHz).

The above antenna patterns are still approximations of the real behavior of a given antenna when used with random noise waveforms. Due to the fact that different frequency components occur in random manner, the actual antenna response will vary with time. An approach to solving this problem is through the use of statistical antenna theory to determine the mean antenna characteristics. Wideband excitation of antenna system impacts the accuracy of the angular measurement by imposing additional fluctuations in the sum and the difference outputs. However, the effects of these variations can be reduced by increasing the observation time and performing signal averaging.

BASIC MONOPULSE MODEL

Figure 2 shows the conceptual model of our proposed random noise phase comparison monopulse system architecture. The two receive antennas with phase centers displaced by 2d feed their signals into a sum and difference network. Unlike the traditional monopulse receiver that mixes two channel signals with a single frequency local oscillator, this architecture correlates the sum and difference channel signals with a delayed replica of transmitted random noise signal $X(t)$ which we denote as $s_d(t)$.

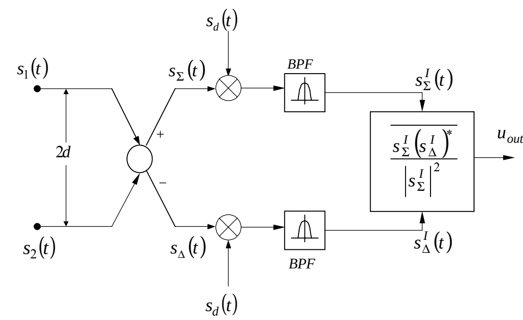

Figure 2: Conceptual model for random noise monopulse system.

In practice, since the delayed transmitted replica is always downconverted to an intermediate frequency (IF) before correlation, phase information is extracted at the IF stage. For simplicity, we can disregard this downconversion process and perform angle estimation directly at baseband. Thus, the bandpass filters in Figure 2 can be temporarily suppressed.

We assume that the target being tracked is far away from antenna system at a range r and off-axis angle θ. The transmitted band-limited white noise signal $X(t)$ can be approximated as the sum of a large number of frequency components across a wide bandwidth, *i.e.,*

$$\hat{X}(t) = \sum_{i=1}^{M} A_i e^{j\omega_i t} \tag{1}$$

In (1), M can be an arbitrary large number depending on the choice of interval ω_0 between adjacent frequency indices, while A_i denotes the random variable satisfying the property of non-zero autocorrelation and zero cross-correlation. Ignoring propagation effects on amplitude of the different frequency components, the received signal at antenna with coordinate value $d_k\ (k = 1,2)$ can be described as

$$X_k(t) = \sum_{i=1}^{M} A_i e^{j\omega_i t} e^{-j\frac{\omega_i}{c}(2r + d_k \sin\theta)} \tag{2}$$

where c is the velocity of light.

Ignoring some amplitude coefficients introduced by the hybrid components, the outputs of sum and difference network are given by

$$\begin{aligned} s_\Sigma(t) &= X_1(t) + X_2(t), \\ s_\Delta(t) &= X_1(t) - X_2(t) \end{aligned} \tag{3}$$

The above sum and difference signals are mixed with the delayed replica $s_d(t)$. The correlation results in both channels are routed through filters that retain the low frequency components around the IF. These filtered outputs are then used to form the complex correlation coefficient in order to generate the final angle estimation. Consequently, the final output of phase comparison monopulse at any given time is obtained as

$$u_{out} = \mathrm{Im}\left(\frac{s_\Sigma^I \left(s_\Delta^I\right)^*}{\left|s_\Sigma^I\right|^2} \right) \tag{4}$$

where Im(.) denotes the imaginary part of the complex argument. Note that s_Σ^I and s_Δ^I are the low frequency outputs in the sum and difference channels respectively.

We assume that the delay line is able to delay the transmitted replica by the precise time according to range 2r, *i.e.,*

$$s_d(t) = \sum_{i=1}^{M} A_i e^{j\omega_i t} e^{-j\frac{\omega_i}{c}\cdot 2r} \tag{5}$$

Then, following the correlation and filtering operations, the range-dependent phase is eliminated, and only the phase containing the angle information remains. Based on the properties of coefficients in (1) and (4), and after simplification, the time average of monopulse output can be expressed as

$$\bar{u}_{out} = \frac{\sum_{i=1}^{M} \overline{A_i^2} \cdot e^{j\frac{\omega_i}{c} d\sin\theta} - \sum_{i=1}^{M} \overline{A_i^2} \cdot e^{-j\frac{\omega_i}{c} d\sin\theta}}{\sum_{i=1}^{M} \overline{A_i^2} \cdot e^{j\frac{\omega_i}{c} d\sin\theta} + \sum_{i=1}^{M} \overline{A_i^2} \cdot e^{-j\frac{\omega_i}{c} d\sin\theta}} \tag{6}$$

Here, $\overline{A}_i$ is the mean value of random amplitude A_i. Recall that the transmit signal is assumed to have constant power density across the total bandwidth $\Delta\omega$. In other words, for each frequency component ω_i, we have

$$\overline{A_i^2} = \begin{cases} \dfrac{\omega_0 S_0}{2\pi} & m = n \\ 0 & m \neq n \end{cases} \tag{7}$$

Thus, (6) can be simplified by taking summations term by term. Assuming that all the frequency components are equally distributed around the center frequency ω_c, and that ω_0 is very small, the final expression derived using (6) and (7) is

$$\bar{u}_{out} \approx \tan\left(\frac{\omega_c}{c} d\sin\theta \right) \tag{8}$$

We see that (8) has the same form as the characteristic curve of a phase comparison monopulse system using a single frequency signal. This means that we can use the random noise waveform to achieve the same angle measurement as conventional monopulse by taking time average, as long as the delay line is ideal.

In actual practice, a real delay line always has finite range resolution, while the moving target will introduce phase errors. These factors decrease system sensitivity, dynamic range and tracking accuracy. For this case, let us consider a "bad delay line", which does not provide any delay and also loses all the frequency components. This is equivalent to saying

$$\begin{aligned} s_\Sigma^I(t) &= \rho s_\Sigma(t), \\ s_\Delta^I(t) &= \rho s_\Delta(t) \end{aligned} \tag{9}$$

Given (2), (3) and (9), we recomputed the monopulse output as shown in (4). This yields

$$\left|\overline{u}'_{out}\right| = \frac{\sum_{i=1}^{M} \overline{A}_i^2 \sin\left(\frac{\omega_i}{c} \cdot 2\,d\sin\theta\right)}{\sum_{i=1}^{M} \overline{A}_i^2 + \sum_{i=1}^{M} \overline{A}_i^2 \cos\left(\frac{\omega_i}{c} \cdot 2\,d\sin\theta\right)} \tag{10}$$

Without loss of generality, we can let M, which is large, be an odd number, *i.e.*, we can assume M=2N+1. This means there are N frequency components below and N frequency components above the center frequency ω_c. Keeping (7) in mind, we can transform (10) into

$$\left|u_{out}\right| = \frac{\sin\left(\frac{\omega_c}{c} 2\,d\sin\theta\right)}{K_c + \cos\left(\frac{\omega_c}{c} 2\,d\sin\theta\right)} \tag{11}$$

where

$$K_c = \frac{M}{1 + \frac{\sin[N\omega_0 d\sin\theta/c]}{\sin[\omega_0 d\sin\theta/c]} \cdot 2\cos[(N+1)\omega_0 d\sin\theta/c]} \tag{12}$$

As the frequency separation ω_0 approaches zero, the above equation more accurately represents the random noise monopulse system. Furthermore,

$$K_c = \frac{M}{1 + 2\,N \cdot \cos\left(\frac{\Delta\omega}{2\,c} d\sin\theta\right)} \tag{13}$$

It can be seen from (11) and (13) that the monopulse output depends on the signal bandwidth. Generally $K_c > 1$ and the monopulse characteristic curve is flattened due to this term. However, if we choose the bandwidth that precisely satisfies

$$\Delta\omega = k \cdot 2\pi \frac{c}{d} \sin\theta \qquad k = 1,2,3,... \tag{14}$$

the cosine term will goes to 1 and

$$K_c \to \frac{M}{1+2\,N} = 1 \tag{15}$$

Then (11) reduces to

$$\left|\overline{u}_{out}\right| = \frac{\sin\left(\frac{\omega_c}{c} 2\,d\sin\theta\right)}{1 + \cos\left(\frac{\omega_c}{c} 2\,d\sin\theta\right)} = \tan\left(\frac{\omega_c}{c} d\sin\theta\right) = \tan\left(\frac{2\pi}{\lambda_c} d\sin\theta\right) \tag{16}$$

Again, this is the same as the single frequency monopulse output.

We can also note that when the signal has narrow bandwidth, *i.e.,* $\Delta\omega \to 0$, (15) and (16) is applicable naturally. Thus we revert to the case of single frequency monopulse.

In summary, even for the worst case, the angle of arrival can still be estimated using the general expression (11), although the receiver sensitivity is lowered. For UWB signals, it is also possible to obtain the same tracking capability as the single frequency monopulse by choosing the appropriate bandwidth.

SYSTEM DESCRIPTION

A complete system has been designed to operate at X-band for demonstrating the random noise phase comparison concept. The radar system adopts a phase coherent heterodyne architecture, and uses two parallel channels to perform single plane tracking. Figure 3 shows the simplified block diagram of this radar.

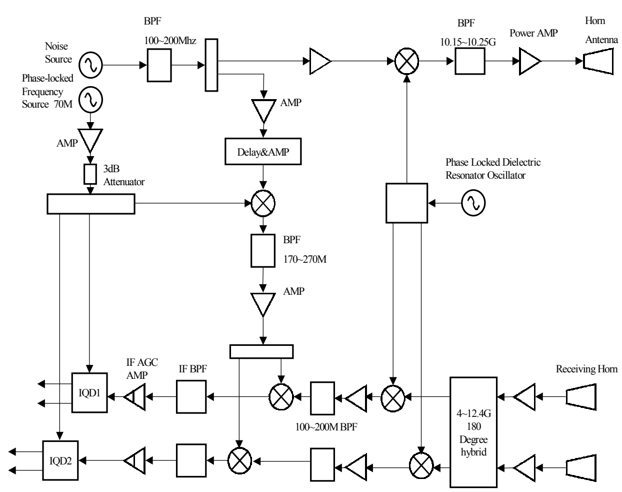

Figure 3: Radar system architecture.

The noise source generates bandlimited random noise signal over the 100-200 MHz frequency range through a bandpass filter. In the transmit channel, this signal is amplified and upconverted to X-band over the 10.15-10.25 GHz frequency range. Another portion of random noise signal is delayed and modulated as the correlation signal $s_d(t)$.

Two receive antennas are placed apart with distance 2d = 30 cm. The signals received by these antennas are fed into the sum and difference network, which is implemented by a 180° hybrid. Signals in the sum and difference channels are first downconverted to the 100-200 MHz frequency range, amplified, filtered, and finally correlated with $s_d(t)$.

The final processing stage consists of extracting the amplitude and phase information in the sum and difference channels. This is implemented using two I/Q detectors. The following signal/data processor digitizes the I/Q signals and performs real-time closed-loop control.

It is interesting to note that the IF bandpass filter actually functions as a time averager that is essential for random noise radar processing. Narrower the passband, longer is the averaging time span. However, some useful information (such as Doppler frequency shift) may be lost if we use too narrow a bandwidth, and a filter with very narrow relative bandwidth is generally difficult to implement. For these reasons, some time averaging is still needed in digital processing stage.

There are some special requirements that make random noise monopulse signal processor different from other noise radars. One is the feedback control capability, and the other is real time processing. The processing scheme is described in Figure 4.

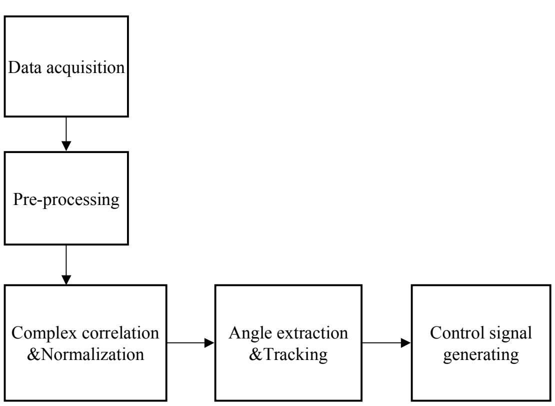

Figure 4: Data processing block diagram.

A real time controller and a multifunction board are adequate for the above tasks. Time constraints must be considered to specify the required hardware/software performance. For range delay and tracking functions, the control cycle should be as short as possible since the target moves continuously. This is a challenge not only for the processor, but also for the delay line subsystem. For angle tracking, the control cycle ΔT must satisfy

$$\dot{\theta} \cdot \Delta T < \theta_M \tag{17}$$

Here, $\dot{\theta}$ denotes angular velocity of the target, θ_M is the linear region limitation of monopulse characteristic curve. If the off-axis angle exceeds θ_M, the angular detector response will saturate, and the antenna controller based on complex correlation will not give correct control signals. More advanced data processing design may use special algorithms to judge the accuracy of the detected angle value, or smooth the angle measurement using tracking filters.

SIMULATIONS AND OBSERVATIONS

Before the implementation of random noise monopulse radar system, it is helpful to predict the dynamic behavior of system architecture through simulations. A rapid and accurate system simulation raises many new requirements for simulation tools. As a comprehensive dynamic system analysis environment, SystemView® is one such software that is suitable for this application. A large system is first divided into subsystems and then specified by tokens and metasystems. Next, components are connected to each other, with some analysis and visualization viewers added. Once the simulation is started, it will go through the system running process in real time.

Figure 5 depicts the random noise waveform generated by a Gaussian noise source and a bandpass filter with different filter bandwidths. Figure 5(a) shows the Gaussian noise waveform generated by the noise source and this simulates an infinite bandwidth. Figures 5(b) and 5(c) show the noise source output filtered using filter bandwidths of 100 MHz and 1 GHz around a center frequency of 10 GHz. These simulations verify that the transmit signal bandwidth can be controlled using the bandpass filter, and that a wider bandwidth adds more fluctuations to the waveform envelope.

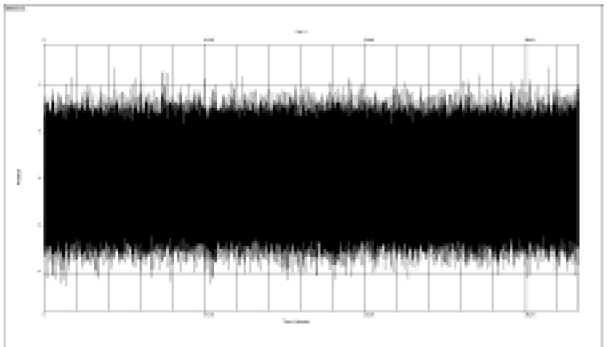

(a) Gaussian white noise simulated by SystemView®

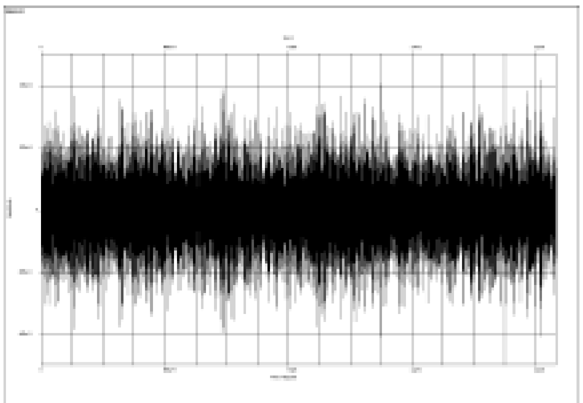

(b) Transmitted random noise waveform filtered using 100 MHz bandwidth BPF

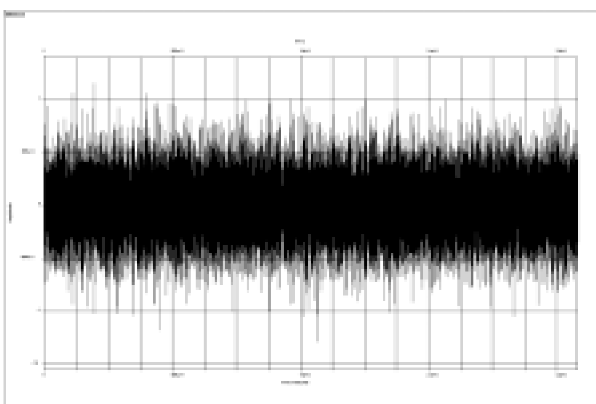

(c) Transmitted random noise waveform filtered using 1 GHz bandwidth BPF

Figure 5: Transmit waveform examples.

The transmitted signals will, in general, be modified by the propagation media such as the atmosphere. Basically, some specially designed filters in one or two token modules can simulate this phenomenon. Also, we can simulate additive interferences and jamming by some other sources and adder modules. The combination of all above factors and range-delay of return waves, received signals in multiple channels can be simulated.

All the radar system components, including sum and difference network (which can be implemented by hybrids or 180° power combiners), amplifiers, mixers, filters, power dividers, etc., are specified with different performance and parameters, and inserted into simulation system as modules. Thus, we can test a broad range of system designs without actual physical implementation. Figure 6 is the top-level view of the simulation system that includes several subsystems.

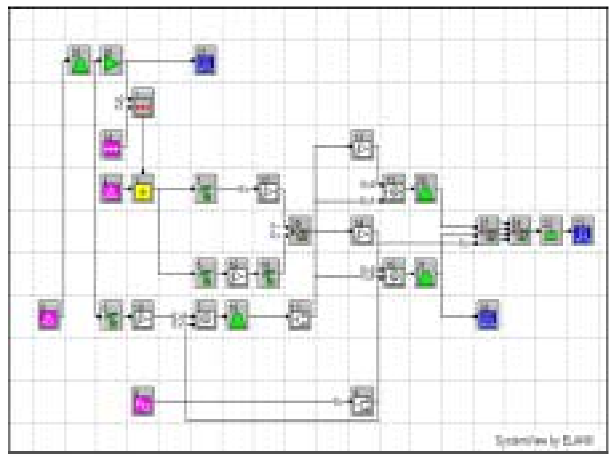

Figure 6: Top level simulation architecture for random noise monopulse.

The architecture in Figure 6 is a “basic” configuration in the sense that it is only used to simulate the measurement of single plane angle associated with the direction of the static target. With more complexity added, it can be expanded to simulate real angle tracking in dual planes.

Figure 7 (a) shows the subsystem architecture of the sum and difference network, Figure 7(b) shows the subsystem architecture of the I/Q detector, and Figure 7(c) shows the subsystem architecture of angle extractor.

One of interesting points of the simulation architecture is the choice of the intermediate frequency (IF) and the bandpass filter following the correlation. These two design factors influence the performance of noise radar dramatically. In the next simulation, the transmitted signal has a bandwidth of 1 GHz and the IF is set at 300 MHz. We then observe the output of correlator with various bandpass filter bandwidths, *viz.*, 2 MHz, 1 MHz, and 100 kHz. These are shown in Figures 8(a), 8(b), and 8(c), respectively.

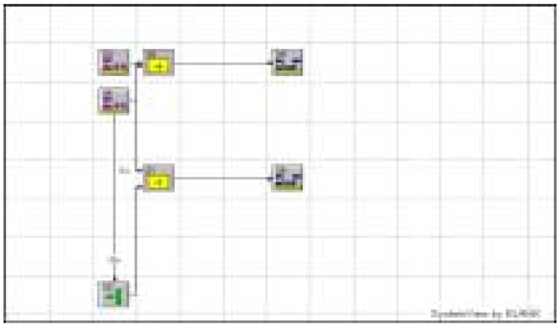

(a) Sum and difference subsystem

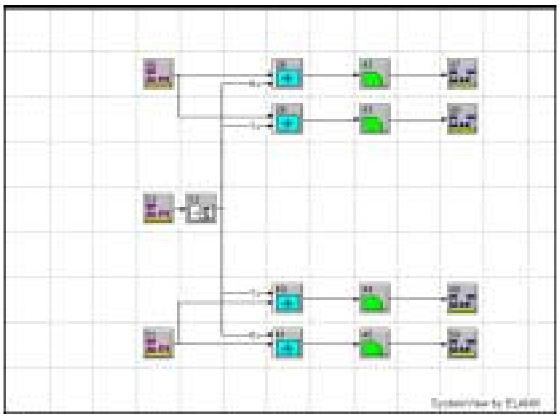

(b) I/Q detector subsystem

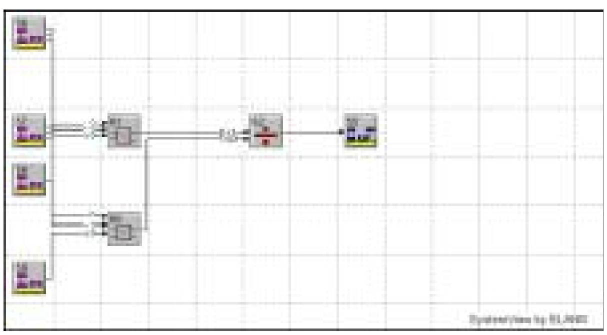

(c) Angle extractor subsystem

Figure 7: Subsystem simulation architectures.

In fact, when the random noise monopulse radar is used for range tracking, what we are interested in the output of correlator is its envelope. We accomplish this by recording the envelope over time and computing its average amplitude. The peak amplitude can be obtained as long as the delay line is matched to the range delay due to the two-way propagation to the target. We can deduce the impact of narrow bandpass filter on this process from Figure 8. We note that decreased

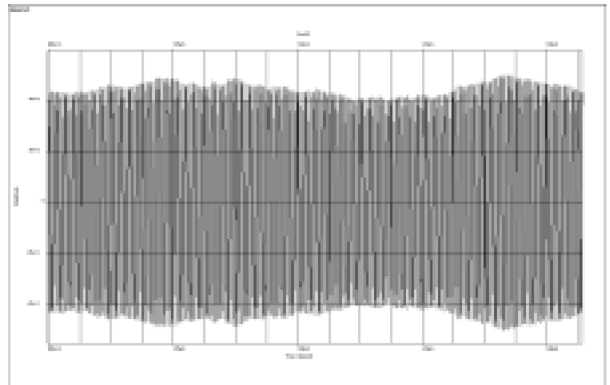

(a) Correlator BW=2 MHz

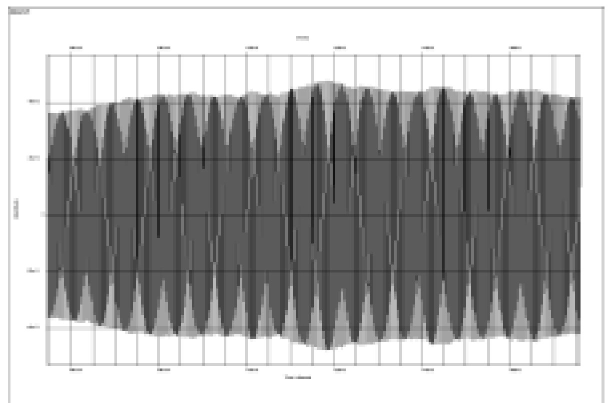

(b) Correlator BW=1 MHz

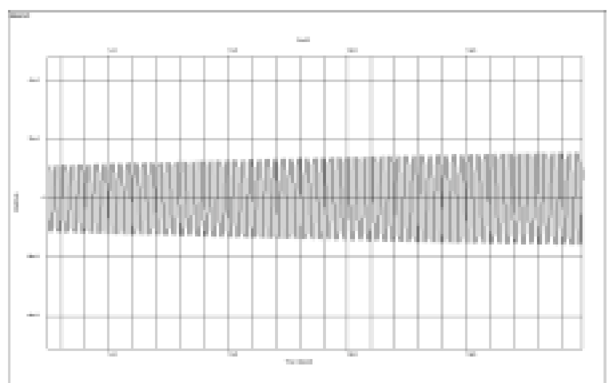

(c) Correlator BW=100 kHz

Figure 8: Real-time output waveform of correlator for different correlator bandwidths.

bandwidth means more integration time; thus, we can obtain a smoother correlation output.

However, we should be aware that too narrow a bandwidth for the filter could become the limiting factor for the system dynamic range. If the target maneuvers abruptly, although the delay line response may follow it in range, the narrowband filter response may lag so much so as to lose the target in angle. Therefore, an optimal system design should partition the time averaging task appropriately between the correlator and the subsequent digital processing system.

Now we turn to the results of angle measurement output. It should be repeated at this point that due to the random nature of transmitted signal, all the measurements are in the sense of time average. Generally, the final output of random noise radar will fluctuate more severely than that of the single frequency system.

Figure 9 compares the system output of single frequency (10 GHz) monopulse and random noise monopulse (IF BW=1 MHz). It is clear that for case of single frequency system, phase information is extracted quickly and output adjusts to a stable state with rapidity, while the random noise monopulse output does not attain very stable states. Rather, it fluctuates around some mean value that is sensitive to off-axis angle of the target.

In order to examine the angular characteristic curve of coherent random noise monopulse, the following simulations are performed for a spacing of 30 cm between the two receive antennas. Figure 10(a) shows the worst case system theoretical output as a function of the transmit bandwidth at a center frequency of 1.5 GHz. The curves for a bandwidth of up to 500 MHz are very similar to that of the single frequency (zero bandwidth) case. In Figure 10(b), the angle of arrival region between –0.25 and +0.25 radians is expanded: the worst-case theoretical curve is shown in dotted while the simulated curve is shown in bold. The difference between these curves is attributed to the non-ideal parameters assumed for the RF components. Figure 10(c) shows curves similar to that in Figure 10(a), except the transmit frequency is now 10 GHz. While the sensitivity is better, the dynamic range is limited, as expected. Figure 10(d) shows the simulated output at 10 GHz.

CONCLUSIONS

This paper introduces an innovative coherent random noise radar system implementing phase comparison monopulse. The theoretical analysis is based on treating random noise waveform as random summation of a great amount of frequency components. The effects of expanded signal bandwidth on receive antenna, receiver architecture, and signal processing are studied. A prototype system is introduced and analyzed. Before the actual implementation of system, a series of

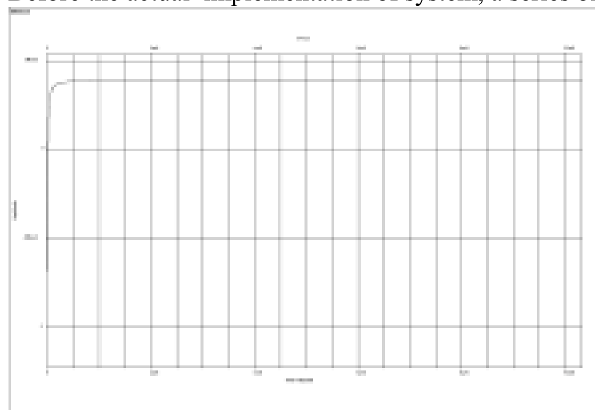

(a) System output of single frequency monopulse

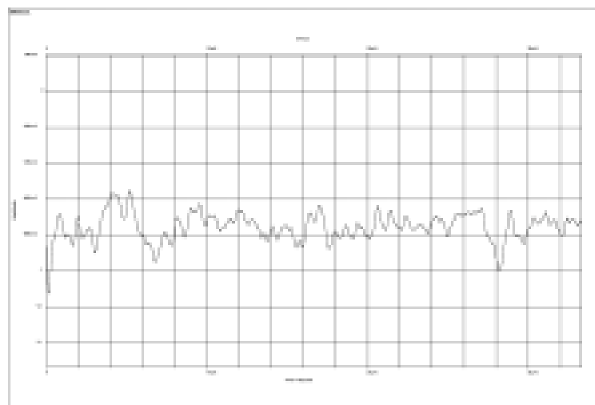

(b) System output of coherent random noise monopulse

Figure 9: Comparison of system output of single frequency monopulse and coherent random noise monopulse.

simulations are performed, and the basic performance measures of the random noise monopulse system are outlined.

Generally speaking, the disadvantages of the random noise monopulse radar are delayed response time, lowered sensitivity, and restricted dynamic range compared to single frequency or narrowband systems operating at the same center frequency. However, they can be overcome greatly by employing high accuracy delay line and high speed time averaging. The system has its main advantage in the fact that it possesses electronic counter counter measures (ECCM) capability, as has been clearly demonstrated by our group[6].

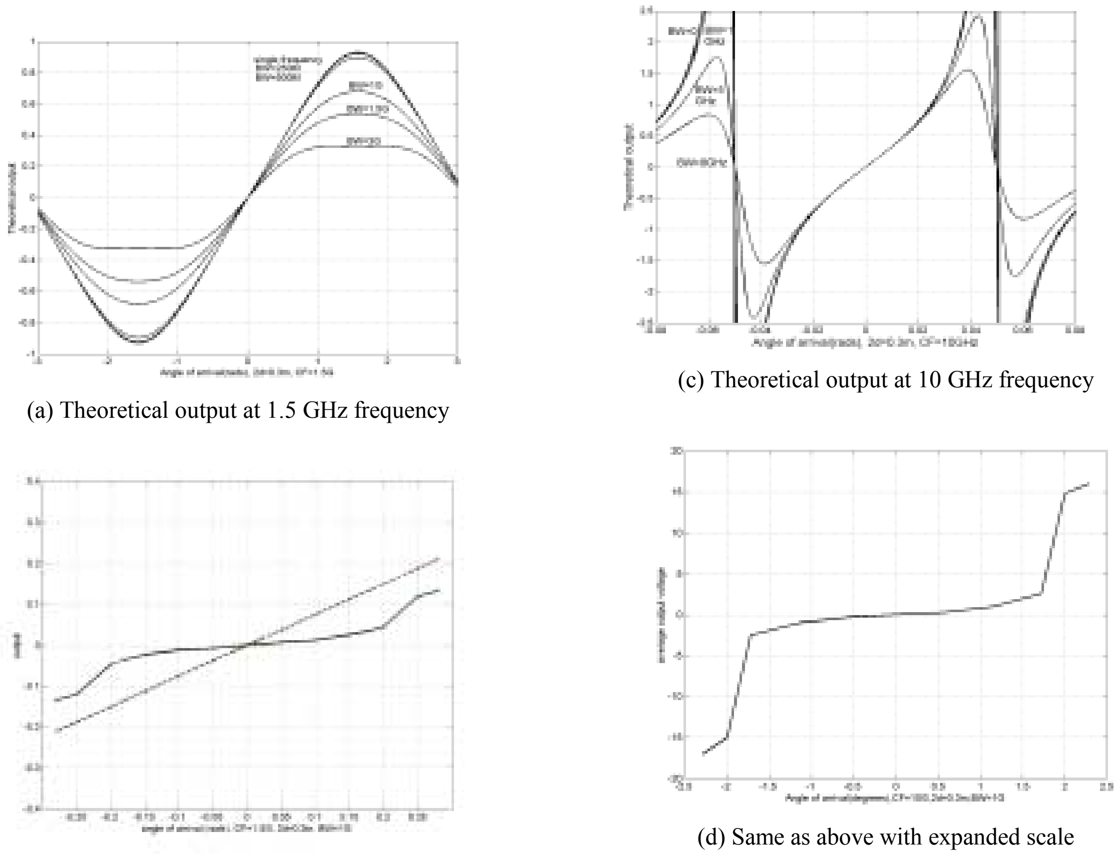

(a) Theoretical output at 1.5 GHz frequency

(c) Theoretical output at 10 GHz frequency

(b) Same as above with expanded scale

(d) Same as above with expanded scale

Figure 10: Theoretical and simulated outputs of the random noise monopulse radar system.

ACKNOWLEDGMENTS

This project is supported by the MDA through the U.S. Army Research Office under contract number DAAD19-01-1-0531. We appreciate helpful comments and suggestions from Dr. Juergen Pohlmann of MDA. Thanks are also due to Yan Zhang and Xiaojian Xu for assistance with the system development and simulation.

REFERENCES

1. R.M. Narayanan, Y. Xu, P.D. Hoffmeyer, and J.O. Curtis, "Design, performance, and applications of a coherent ultra-wideband random noise radar," *Optical Engineering,* **37**(6): 1855-1869, June 1998.
2. R.M. Narayanan and M. Dawood, "Doppler estimation using a coherent ultra-wideband random noise radar," *IEEE Transactions on Antennas & Propagation,* **48**(6): 868-878, June 2000.
3. D.S. Garmatyuk and R.M. Narayanan, "Ultrawideband noise synthetic aperture radar: theory and experiment," *Digest of the 1999 IEEE Antennas & Propagation Symposium,* Orlando, FL, **4**: 2226-2229, July 1999.
4. D.C. Bell and R.M. Narayanan, "ISAR imaging using a coherent ultra-wideband random noise radar system," *Optical Engineering,* **40**(11)**:** 2612-2622, November 2001.
5. R.M. Narayanan, R.D. Mueller, and R.D. Palmer, "Random noise radar interferometry," *Proceedings of the SPIE Conference on Radar Processing, Technology, and Applications,* Denver, CO, **2845**: 75-82, August 1996.
6. D.S. Garmatyuk and R.M. Narayanan, "ECCM capabilities of an ultra-wideband bandlimited random noise imaging radar," *IEEE Transactions on Aerospace & Electronic Systems,* **38**: in press, 2002.